ISSN 1948-9366 (online)

World Journal of *Gastrointestinal Surgery*

World J Gastrointest Surg 2024 July 27; 16(7): 1956-2364

Published by Baishideng Publishing Group Inc

World Journal of
Gastrointestinal Surgery

Contents

Monthly Volume 16 Number 7 July 27, 2024

EDITORIAL

1956 Unveiling the potential of electrocautery-enhanced lumen-apposing metal stents in endoscopic ultrasound-guided biliary drainage

Chisthi MM

1960 Minimally invasive pelvic exenteration for primary or recurrent locally advanced rectal cancer: A glimpse into the future

Kehagias D, Lampropoulos C, Kehagias I

1965 Endoscopic submucosal dissection for early gastric cancer: A major challenge for the west

Schlottmann F

1969 Impact of immunotherapy on liver metastasis

Fu Z, Wang MW, Liu YH, Jiao Y

1973 Occurrence and prevention of incisional hernia following laparoscopic colorectal surgery

Wu XW, Yang DQ, Wang MW, Jiao Y

1981 Role of endoscopic-ultrasound-guided biliary drainage with electrocautery-enhanced lumen-apposing metal stent for palliation of malignant biliary obstruction

Deliwala SS, Qayed E

REVIEW

1986 Pancreatic pseudocyst: The past, the present, and the future

Koo JG, Liau MYQ, Kryvoruchko IA, Habeeb TA, Chia C, Shelat VG

ORIGINAL ARTICLE

Case Control Study

2003 Diagnostic significance of serum levels of serum amyloid A, procalcitonin, and high-mobility group box 1 in identifying necrotising enterocolitis in newborns

Guo LM, Jiang ZH, Liu HZ, Zhang L

Retrospective Cohort Study

2012 Clinical efficacy and safety of double-channel anastomosis and tubular gastroesophageal anastomosis in gastrectomy

Liu BY, Wu S, Xu Y

2023 Application of radioactive iodine-125 microparticles in hepatocellular carcinoma with portal vein embolus

Meng P, Ma JP, Huang XF, Zhang KL

Contents

Retrospective Study

2031 Reproducibility study of intravoxel incoherent motion and apparent diffusion coefficient parameters in normal pancreas

Liu X, Wang YF, Qi XH, Zhang ZL, Pan JY, Fan XL, Du Y, Zhai YM, Wang Q

2040 Weight regain after intragastric balloon for pre-surgical weight loss

Abbitt D, Choy K, Kovar A, Jones TS, Wikiel KJ, Jones EL

2047 Retrospective analysis based on a clinical grading system for patients with hepatic hemangioma: A single center experience

Zhou CM, Cao J, Chen SK, Tuxun T, Apaer S, Wu J, Zhao JM, Wen H

2054 Spleen volume is associated with overt hepatic encephalopathy after transjugular intrahepatic portosystemic shunt in patients with portal hypertension

Zhao CJ, Ren C, Yuan Z, Bai GH, Li JY, Gao L, Li JH, Duan ZQ, Feng DP, Zhang H

2065 Evaluation of the clinical effects of atropine in combination with remifentanil in children undergoing surgery for acute appendicitis

Li YJ, Chen YY, Lin XL, Zhang WZ

2073 The combined detection of carcinoembryonic antigen, carcinogenic antigen 125, and carcinogenic antigen 19-9 in colorectal cancer patients

Gong LZ, Wang QW, Zhu JW

2080 Clinical efficacy of laparoscopic cholecystectomy plus cholangioscopy for the treatment of cholecystolithiasis combined with choledocholithiasis

Liu CH, Chen ZW, Yu Z, Liu HY, Pan JS, Qiu SS

2088 Association between operative position and postoperative nausea and vomiting in patients undergoing laparoscopic sleeve gastrectomy

Li ZP, Song YC, Li YL, Guo D, Chen D, Li Y

2096 Preoperative albumin-bilirubin score predicts short-term outcomes and long-term prognosis in colorectal cancer patients undergoing radical surgery

Diao YH, Shu XP, Tan C, Wang LJ, Cheng Y

2106 Association of preoperative antiviral treatment with incidences of post-hepatectomy liver failure in hepatitis B virus-related hepatocellular carcinoma

Wang X, Lin ZY, Zhou Y, Zhong Q, Li ZR, Lin XX, Hu MG, He KL

2119 Effect of rapid rehabilitation nursing on improving clinical outcomes in postoperative patients with colorectal cancer

Song JY, Cao J, Mao J, Wang JL

2127 Interaction between the albumin-bilirubin score and nutritional risk index in the prediction of post-hepatectomy liver failure

Qin FF, Deng FL, Huang CT, Lin SL, Huang H, Nong JJ, Wei MJ

World Journal of Gastrointestinal Surgery

Monthly Volume 16 Number 7 July 27, 2024

Contents

2135 Effectiveness of magnetic resonance imaging and spiral computed tomography in the staging and treatment prognosis of colorectal cancer

Bai LN, Zhang LX

2145 Correlation between abdominal computed tomography signs and postoperative prognosis for patients with colorectal cancer

Yang SM, Liu JM, Wen RP, Qian YD, He JB, Sun JS

2157 Study on the occurrence and influencing factors of gastrointestinal symptoms in hemodialysis patients with uremia

Yuan D, Wang XQ, Shao F, Zhou JJ, Li ZX

2167 "Hepatic hilum area priority, liver posterior first": An optimized strategy in laparoscopic resection for type III-IV hilar cholangiocarcinoma

Hu XS, Wang Y, Pan HT, Zhu C, Chen SL, Zhou S, Liu HC, Pang Q, Jin H

2175 Impact of nutritional support on immunity, nutrition, inflammation, and outcomes in elderly gastric cancer patients after surgery

Chen XW, Guo XC, Cheng F

2183 Therapeutic effects of Buzhong Yiqi decoction in patients with spleen and stomach qi deficiency after routine surgery and chemotherapy for colorectal cancer

Hu Q, Chen XP, Tang ZJ, Zhu XY, Liu C

2194 Influencing factors and risk prediction model for emergence agitation after general anesthesia for primary liver cancer

Song SS, Lin L, Li L, Han XD

2202 Potential applications of single-incision laparoscopic totally preperitoneal hernioplasty

Wang XJ, Fei T, Xiang XH, Wang Q, Zhou EC

2211 Clinical significance of preoperative nutritional status in elderly gastric cancer patients undergoing radical gastrectomy: A single-center retrospective study

Zhao XN, Lu J, He HY, Ge SJ

2221 Establishment and validation of a predictive model for peripherally inserted central catheter-related thrombosis in patients with liver cancer

Chen XF, Wu HJ, Li T, Liu JB, Zhou WJ, Guo Q

Observational Study

2232 Effect of information-motivation-behavioral skills model based perioperative nursing on pain in patients with gallstones

Ma L, Yu Y, Zhao BJ, Yu YN, Li Y

2242 Postoperative body weight change and its influencing factors in patients with gastric cancer

Li Y, Huang LH, Zhu HD, He P, Li BB, Wen LJ

2255 Cost burden following esophagectomy: A single centre observational study

Buchholz V, Lee DK, Liu DS, Aly A, Barnett SA, Hazard R, Le P, Kioussis B, Muralidharan V, Weinberg L

World Journal of Gastrointestinal Surgery

Monthly Volume 16 Number 7 July 27, 2024

Contents

Randomized Controlled Trial

2270 Effectiveness of colonoscopy, immune fecal occult blood testing, and risk-graded screening strategies in colorectal cancer screening

Xu M, Yang JY, Meng T

Clinical and Translational Research

2281 Construction of prognostic markers for gastric cancer and comprehensive analysis of pyroptosis-related long non-coding RNAs

Wang Y, Li D, Xun J, Wu Y, Wang HL

Basic Study

2296 Yangyin Huowei mixture alleviates chronic atrophic gastritis by inhibiting the IL-10/JAK1/STAT3 pathway

Xie SS, Zhi Y, Shao CM, Zeng BF

2308 Impacts of different pancreatic resection ranges on endocrine function in *Suncus murinus*

Li RJ, Yang T, Zeng YH, Natsuyama Y, Ren K, Li J, Nagakawa Y, Yi SQ

SYSTEMATIC REVIEWS

2319 Impact of frailty on postoperative outcomes after hepatectomy: A systematic review and meta-analysis

Lv YJ, Xu GX, Lan JR

CASE REPORT

2329 Multidisciplinary management of ulcerative colitis complicated by immune checkpoint inhibitor-associated colitis with life-threatening gastrointestinal hemorrhage: A case report

Hong N, Wang B, Zhou HC, Wu ZX, Fang HY, Song GQ, Yu Y

2337 Sequential bowel necrosis and large gastric ulcer in a patient with a ruptured femoral artery: A case report

Wang P, Wang TG, Yu AY

2343 Colon signet-ring cell carcinoma with chylous ascites caused by immunosuppressants following liver transplantation: A case report

Li Y, Tai Y, Wu H

2351 Misdiagnosis of hemangioma of left triangular ligament of the liver as gastric submucosal stromal tumor: Two case reports

Wang JJ, Zhang FM, Chen W, Zhu HT, Gui NL, Li AQ, Chen HT

LETTER TO THE EDITOR

2358 Revolutionizing palliative care: Electrocautery-enhanced lumen-apposing metal stents in endoscopic-ultrasound-guided biliary drainage for malignant obstructions

Onteddu NKR, Mareddy NSR, Vulasala SSR, Onteddu J, Virarkar M

World Journal of Gastrointestinal Surgery

Monthly Volume 16 Number 7 July 27, 2024

Contents

2362 Preservation of superior rectal artery in laparoscopic colectomy: The best choice for slow transit constipation?

Liu YL, Liu WC

World Journal of Gastrointestinal Surgery

Monthly Volume 16 Number 7 July 27, 2024

Contents

ABOUT COVER

Peer Reviewer of *World Journal of Gastrointestinal Surgery*, Hideki Aoki, MD, PhD, Chief Doctor, Surgeon, Department of Surgery, Iwakuni Clinical Center, Iwakuni 740-8510, Japan. aoki.hideki.hy@mail.hosp.go.jp

AIMS AND SCOPE

The primary aim of *World Journal of Gastrointestinal Surgery* (*WJGS*, *World J Gastrointest Surg*) is to provide scholars and readers from various fields of gastrointestinal surgery with a platform to publish high-quality basic and clinical research articles and communicate their research findings online.

WJGS mainly publishes articles reporting research results and findings obtained in the field of gastrointestinal surgery and covering a wide range of topics including biliary tract surgical procedures, biliopancreatic diversion, colectomy, esophagectomy, esophagostomy, pancreas transplantation, and pancreatectomy, *etc*.

INDEXING/ABSTRACTING

The *WJGS* is now abstracted and indexed in Science Citation Index Expanded (SCIE, also known as SciSearch®), Current Contents/Clinical Medicine, Journal Citation Reports/Science Edition, PubMed, PubMed Central, Reference Citation Analysis, China Science and Technology Journal Database, and Superstar Journals Database. The 2024 Edition of Journal Citation Reports® cites the 2023 journal impact factor (JIF) for *WJGS* as 1.8; JIF without journal self cites: 1.7; 5-year JIF: 1.9; JIF Rank: 123/290 in surgery; JIF Quartile: Q2; and 5-year JIF Quartile: Q3.

RESPONSIBLE EDITORS FOR THIS ISSUE

Production Editor: *Zi-Hang Xu*; **Production Department Director:** *Xiang Li*; **Cover Editor:** *Jia-Ru Fan*.

NAME OF JOURNAL
World Journal of Gastrointestinal Surgery

ISSN
ISSN 1948-9366 (online)

LAUNCH DATE
November 30, 2009

FREQUENCY
Monthly

EDITORS-IN-CHIEF
Peter Schemmer

EDITORIAL BOARD MEMBERS
https://www.wjgnet.com/1948-9366/editorialboard.htm

PUBLICATION DATE
July 27, 2024

COPYRIGHT
© 2024 Baishideng Publishing Group Inc

INSTRUCTIONS TO AUTHORS
https://www.wjgnet.com/bpg/gerinfo/204

GUIDELINES FOR ETHICS DOCUMENTS
https://www.wjgnet.com/bpg/GerInfo/287

GUIDELINES FOR NON-NATIVE SPEAKERS OF ENGLISH
https://www.wjgnet.com/bpg/gerinfo/240

PUBLICATION ETHICS
https://www.wjgnet.com/bpg/GerInfo/288

PUBLICATION MISCONDUCT
https://www.wjgnet.com/bpg/gerinfo/208

ARTICLE PROCESSING CHARGE
https://www.wjgnet.com/bpg/gerinfo/242

STEPS FOR SUBMITTING MANUSCRIPTS
https://www.wjgnet.com/bpg/GerInfo/239

ONLINE SUBMISSION
https://www.f6publishing.com

W J G S

World Journal of Gastrointestinal Surgery

Submit a Manuscript: https://www.f6publishing.com

World J Gastrointest Surg 2024 July 27; 16(7): 2031-2039

DOI: 10.4240/wjgs.v16.i7.2031

ISSN 1948-9366 (online)

ORIGINAL ARTICLE

Retrospective Study

Reproducibility study of intravoxel incoherent motion and apparent diffusion coefficient parameters in normal pancreas

Xiang Liu, Yi-Feng Wang, Xiao-Hui Qi, Zhi-Lei Zhang, Jiang-Yang Pan, Xue-Li Fan, Yu Du, Ying-Min Zhai, Qi Wang

Specialty type: Gastroenterology and hepatology

Provenance and peer review: Unsolicited article; Externally peer reviewed.

Peer-review model: Single blind

Peer-review report's classification

Scientific Quality: Grade C

Novelty: Grade B

Creativity or Innovation: Grade B

Scientific Significance: Grade B

P-Reviewer: Huntsman DG, Canada

Received: February 22, 2024

Revised: April 11, 2024

Accepted: May 27, 2024

Published online: July 27, 2024

Processing time: 151 Days and 7.1 Hours

Xiang Liu, Yi-Feng Wang, Xiao-Hui Qi, Zhi-Lei Zhang, Jiang-Yang Pan, Xue-Li Fan, Yu Du, Ying-Min Zhai, Qi Wang, Department of CT and MRI, The Fourth Hospital of Hebei Medical University, Shijiazhuang 050000, Hebei Province, China

Corresponding author: Qi Wang, Doctor, Chief Doctor, Department of CT and MRI, The Fourth Hospital of Hebei Medical University, No. 12 Jiankang Road, Shijiazhuang 050000, Hebei Province, China. 47400852@hebmu.edu.cn

Abstract

BACKGROUND

The consistency of pancreatic apparent diffusion coefficient (ADC) values and intravoxel incoherent motion (IVIM) parameter values across different magnetic resonance imaging (MRI) devices significantly impacts the patient's diagnosis and treatment.

AIM

To explore consistency in image quality, ADC values, and IVIM parameter values among different MRI devices in pancreatic examinations.

METHODS

This retrospective study was approved by the local ethics committee, and informed consent was obtained from all participants. In total, 22 healthy volunteers (10 males and 12 females) aged 24-61 years (mean, 28.9 ± 2.3 years) underwent pancreatic diffusion-weighted imaging using 3.0T MRI equipment from three vendors. Two independent observers subjectively scored image quality and measured the pancreas's overall ADC values and signal-to-noise ratios (SNRs). Subsequently, regions of interest (ROIs) were delineated for the IVIM parameters (true diffusion coefficient, pseudo-diffusion coefficient, and perfusion fraction) using post-processing software. These ROIs were on the head, body, and tail of the pancrease. The subjective image ratings were assessed using the kappa consistency test. Intraclass correlation coefficients (ICCs) and mixed linear models were used to evaluate each device's quantitative parameter values. Finally, a pairwise analysis of IVIM parameter values across each device was performed using Bland-Altman plots.

RESULTS

The Kappa value for the subjective ratings of the different observers was 0.776 (P < 0.05). The ICC values for inter-observer and intra-observer agreements for the quantitative parameters were 0.803 [95% confidence interval (CI): 0.684-0.880] and 0.883 (95%CI: 0.760-0.945), respectively (P < 0.05). The ICCs for the SNR between different devices was comparable (P > 0.05), and the ICCs for the ADC values from different devices were 0.870, 0.707, and 0.808, respectively (P < 0.05). Notably, only a few statistically significant inter-device agreements were observed for different IVIM parameters, and among those, the ICC values were generally low. The mixed linear model results indicated differences (P < 0.05) in the f-value for the pancreas head, D-value for the pancreas body, and D-value for the pancreas tail obtained using different MRI machines. The Bland-Altman plots showed significant variability at some data points.

CONCLUSION

ADC values are consistent among different devices, but the IVIM parameters' repeatability is moderate. Therefore, the variability in the IVIM parameter values may be associated with using different MRI machines. Thus, caution should be exercised when using IVIM parameter values to assess the pancreas.

Key Words: Intravoxel incoherent motion; Pancreas; Image quality; Consistency test

Core Tip: The purpose of this study was to investigate whether the intravoxel incoherent motion (IVIM) parameter values of the normal pancreas are consistent when imaging with different magnetic resonance imaging (MRI) devices, and it was found that the variability of IVIM parameter values may be related to the use of different MRI machines.

Citation: Liu X, Wang YF, Qi XH, Zhang ZL, Pan JY, Fan XL, Du Y, Zhai YM, Wang Q. Reproducibility study of intravoxel incoherent motion and apparent diffusion coefficient parameters in normal pancreas. *World J Gastrointest Surg* 2024; 16(7): 2031-2039

URL: https://www.wjgnet.com/1948-9366/full/v16/i7/2031.htm

DOI: https://dx.doi.org/10.4240/wjgs.v16.i7.2031

INTRODUCTION

The microscopic movement of water in biological tissues typically includes the diffusion of water molecules and microcirculation perfusion. Diffusion-weighted imaging (DWI) is sensitive to proton displacement due to random Brownian motion and the overall displacement of protons within the capillaries[1]. In 1986, Le Bihan *et al*[2] introduced the concept of intravoxel incoherent motion (IVIM), which uses a bi-exponential decay model to capture tissue displacements attributed to microcirculatory perfusion and water molecule diffusion. IVIM involves acquiring DWI sequences with multiple b-values, which are processed using a bi-exponential model to obtain quantitative parameters, including the true diffusion coefficient (D), pseudo-diffusion coefficient associated with microperfusion, and perfusion fraction (f). These parameters are used to quantitatively analyze human tissues' microstructural and pathophysiological status.

The increased magnetic resonance imaging (MRI) field strength and related technological innovations have recently led to a steady growth in IVIM analysis research. IVIM analysis is used to study human physiological and pathological processes, including the differentiation of benign and malignant tumors, pathological grading of malignant tumors, prognosis prediction, and many other aspects[3-6]. Moreover, research on IVIM sequence application in pancreatic diseases has also increased. IVIM multi-parameter analysis provides quantitative parameters for assessing pancreatic fat degeneration and fibrosis[7] and distinguishes between normal pancreatic tissue, pancreatic cancer, and pancreatic neuroendocrine tumors[8-10]. Furthermore, it has shown significant value for assessing the degree of pancreatic cancer differentiation[11] and predicting pancreatic cancer resectability[12].

A prerequisite for translating this growing research interest in IVIM multi-parameter analysis into clinical applications is its repeatability in different clinical settings. In clinical practice, the pancreas, a retroperitoneal organ, is often affected by respiratory motion and peristalsis during imaging. Moreover, different hospitals may have various MRI equipment, and even within the same hospital, different MRI devices may be introduced. The consistency of pancreatic IVIM parameter values across different MRI devices significantly impacts the patient's diagnosis and treatment. Therefore, this study aimed to investigate whether the IVIM parameter values of the normal pancreas are consistent when imaged using different MRI devices.

MATERIALS AND METHODS

Study subjects

This study included 22 physically healthy volunteers (10 males and 12 females) aged 24-61 years (mean: 28.9 ± 2.3 years). The inclusion criteria were as follows: (1) No history of drug or alcohol abuse; (2) no history of pancreatitis, diabetes, alcoholism, or abdominal surgery; and (3) no MRI contraindications (such as pacemaker implantation, metal implants, and claustrophobia). The exclusion criteria were as follows: (1) Failure to complete the DWI image examination; and (2) poor image quality (such as motion artifacts), which is insufficient for analysis. This prospective study was approved by the local ethics committee, and informed consent was obtained from all participants.

Scanning technique

Before the examination, each volunteer fasted for 4-6 h. Subsequently, they were examined sequentially using three different 3.0T MRI devices denoted as A for the 3.0T Siemens Skyra, B for the 3.0T Philips Ingenia CX, and C for the domestic 3.0T United Imaging 780. In total, 66 examinations were performed (three examinations per volunteer). The volunteers were placed in a supine position, and the scanning range included the entire pancreas. The scan slice thickness was 5 mm for all MRI devices, and the scan sequences included T1-weighted Dixon, T2-weighted fat suppression, and plain IVIM sequences. IVIM sequence parameter values were calculated based on 12 *b*-values: 0, 10, 20, 30, 40, 60, 80, 100, 200, 500, 800, and 1200 s/mm². The number of excitations (NEX) for different *b*-values was as follows: NEX = 1 for *b*-values of 0-100 s/mm², NEX = 2 for 200 s/mm², NEX = 3 for 500 s/mm², NEX = 5 for 800 s/mm², and NEX = 6 for 1200 s/mm². The settings of the different machines are listed in Table 1.

Image analysis and data measurement

After completing the MRI examinations, two professionally trained radiologists experienced in diagnostic imaging subjectively and objectively assessed the images at a *b*-value of 1200 s/mm². A 5-point rating scale was used for the subjective assessment of image quality, where 1 point represents the poorest and 5 points represent the best, with increasing degrees of quality from points 1 to 5.

Signal-to-noise ratio (SNR) is an objective assessment metric for image quality; it is calculated using the formula SNR = [S - average value (Sb)]/SD, where S represents the average signal value within the pancreatic region of interest (ROI), Sb represents the average background signal value, and SD represents the standard deviation of the signal within the pancreatic ROI. Images with a *b*-value of 1200 s/mm² were selected to measure the pancreatic ROI signal average values, and circular ROIs with an area of approximately 50 mm² were drawn at three locations: The pancreatic head (PaH), pancreatic body (PaB), and pancreatic tail (PaT). The average values and standard deviations of the signal for each ROI were recorded, and the average values of the three ROIs were calculated. Circular regions were drawn in each of the four corners within the imaging field to measure the background signal values. Each region’s average signal values were recorded, and the Sb for the four regions was calculated. The SNR of the images was calculated using the formula above.

Parameter values were measured on different devices at their respective post-processing workstations. Images with *b*-values of 0 and 1200 s/mm² were selected to generate the apparent diffusion coefficient (ADC) maps. The ADC values were measured separately for the PaH, PaB, and PaT, and the overall average ADC value for the pancreas was calculated. The delineation of the IVIM sequence ROI and the calculation of the parameter values were performed using the MITK-diffusion post-processing software of different devices to obtain the true *D*, false diffusion coefficient (*D**), and *f* values. *D* represents the effect of pure molecular diffusion within a voxel, *D** represents the diffusion effect associated with microcirculation perfusion, and *f* represents the volume fraction of the diffusion effects associated with microcirculation perfusion within a voxel, expressed as a percentage. Owing to the differences in the IVIM parameter values in different parts of the pancreas[13], the ROIs were delineated at the best-displayed levels for the PaH, PaB, and PaT. ROIs were drawn on axial images at *b* = 0 s/mm², with an area of 50 mm². The common bile duct and main pancreatic duct were avoided during the delineation. Notably, all quantitative parameter measurements were performed by two experienced radiologists, and one repeated the measurements for all quantitative parameters 1 mo later.

Statistical processing

SAS 9.4 software, R language, and SPSS 26.0 were used for data collection and statistical analyses. Kappa analysis was used to compare the consistency of the subjective image quality scores between the observers. Kappa ≥ 0.75 indicated good consistency, 0.75 > Kappa ≥ 0.4 indicated general consistency, and kappa < 0.4 indicated poor consistency between the two observers. The intraclass correlation coefficient (ICC) was used to analyze the parameters between different observers and between two measurements from the same observer. Good consistency was indicated by ≥ 0.75, and 0.40-0.75 indicated moderate consistency. A value of < 0.40 indicated poor consistency.

The consistency of image SNR, ADC, and IVIM parameter values among different MRI devices was analyzed using ICC. The mean ± SD method was used to describe the IVIM parameter data between the different MRI devices. Differences between different devices were compared using a mixed linear model, and *post-hoc* pairwise comparisons were adjusted using the Bonferroni method, where the adjusted *P*-values were calculated by multiplying the original *P*-values by 3. Finally, Bland-Altman plots were used to evaluate the consistency of IVIM measurements across different devices. All statistical analyses and graphical representations were performed using GraphPad Prism 9.3 software, and statistical significance was set at $P < 0.05$.

Table 1 Parameter settings for different machines

Model	TR (ms)	TE (ms)	FOV (mm)	Matrix	Lamination thickness (mm)	Scanning time (min:s)
A	6700	63	380 × 306	108 × 134	5	8:35
B	1897	75	380 × 297	128 × 98	5	3:36
C	4294	67	380 × 300	128 × 100	5	4:57

RESULTS

Consistency analysis between different observers

The Kappa value for the subjective image quality assessment among the observers was 0.776 (P < 0.05). The ICC for all quantitative parameter values among different observers was 0.803 [95% confidence interval (CI): 0.684-0.880, P < 0.05]. The ICC for the quantitative parameter values measured by the same observer on two different occasions was 0.883 (95%CI: 0.760-0.945, P < 0.05).

Consistency analysis between different devices

Consistency analysis results of SNR and ADC values between different devices: The mean SNR values for MRI devices A, B, and C were 14.2 ± 3.1, 11.9 ± 2.4, and 15.5 ± 3.6, respectively. Device C had the highest SNR among the three devices. The ICC between different devices was not significant (P > 0.05; Table 2). The ICCs of the ADC values of devices A, B, and C were 0.870, 0.707, and 0.808, respectively (P < 0.05) (Table 2). The ICC between devices A and C was between 0.4 and 0.75, indicating that the repeatability of ADC value measurements between the two devices is moderate. However, for the comparisons between devices A and B and between devices B and C, the ICC was > 0.75, indicating good repeatability in ADC measurements between these device pairs.

ICC results of IVIM parameters between different devices: The D, $D*$, and f values of the PaH, PaB, and PaT on different devices are statistically described using box plots (Figure 1). According to the ICC results, only a few differences between the devices were statistically significant. Devices A and B were statistically significant only for the f value of the PaT, with an ICC of 0.531 (P < 0.05). The difference in the D value of the PaB between devices A and C was statistically significant, and the ICC was 0.683 (P < 0.05). Devices B and C had more statistically significant differences. The two devices were statistically significant for the D and $D*$ values of the PaH, D value of the PaB, and D value of the PaT. The ICC obtained was 0.728, 0.578, 0.551, and 0.908, respectively (P < 0.05). Similarly, from the ICC results, in the above statistically significant items, only the ICC of the D values of the PaT on devices B and C were > 0.75, and the ICC of the remaining items were between 0.4 and 0.75 (Table 2 and Figure 2).

Analysis of differences in IVIM parameter values among different pancreatic regions on different machines: The mixed linear model analysis results showed differences in the f value of the PaH, the D value of the PaB, and the $D*$ value of the PaT among different devices (P < 0.05). The f value of the PaH on device C was lower than those on devices A and B (P < 0.05). The D value of the PaB on device C was higher than those on devices A and B (P < 0.05). The $D*$ value of the PaT on device B was lower than that on device A (P < 0.05) (Table 3).

Bland-Altman plot analysis between different machines: In a Bland-Altman plot, if the majority of data points fall within the 95% limits of agreement (between the two dashed lines representing the mean ± 1.96 times the SD), and the maximum difference is clinically acceptable, it can be considered that the two methods exhibit good agreement and can be used interchangeably. As shown in Figure 3, there was one point beyond the 95% limits of agreement for devices A and B (orange), one point for devices A and C (purple), and two points for devices B and C (dark green).

DISCUSSION

With advancements in MRI equipment and technology, research on IVIM and its potential clinical applications has increased. This necessitates a systematic assessment of the variability of the measured diffusion parameters. IVIM is a novel MRI technique used for the non-invasive evaluation of molecular diffusion and perfusion within living tissues. It is considered an ideal method for the non-invasive assessment and differentiation of pancreatic cancer[14].

The image quality and parameter values of IVIM are influenced by various factors, such as the magnetic field strength, choice of b-values, selection of breathing techniques, image post-processing methods, and the use of MRI equipment manufactured by different vendors. Previous studies on the consistency of IVIM parameter values have primarily focused on exploring the impact of different breathing techniques, various b-values, and the selection of optimal b-values on ADC or IVIM parameters within the same device[15-17]. However, there have been relatively few studies on the consistency of IVIM parameter values between different devices. Therefore, our study used three MRI machines with a magnetic field strength of 3.0T, identical b-value selection, and respiratory-triggered scanning. The final step involved delineating ROIs of the same size (50 mm²) on images from all machines, minimizing interference from other factors to some extent.

Table 2 Intraclass correlation coefficient results of parameter values in different parts of the pancreas between different devices

	Machine A *vs* machine B		Machine A *vs* machine C		Machine B *vs* machine C	
	ICC (95%CI)	*P* value	ICC (95%CI)	*P* value	ICC (95%CI)	*P* value
D in PaH	0.274 (-0.731, 0.697)	0.232	0.342 (-0.411, 0.712)	0.145	0.728 (0.358, 0.886)	0.002
*D** in PaH	-0.186 (-1.545, 0.482)	0.670	0.27 (-0.611, 0.685)	0.220	0.578 (0.02, 0.822)	0.022
f in PaH	-0.209 (-1.818, 0.491)	0.673	0.173 (-0.386, 0.582)	0.272	0.19 (-0.541, 0.622)	0.274
D in PaB	0.456 (-0.332, 0.776)	0.089	0.683 (-0.026, 0.886)	0.028	0.551 (-0.079, 0.814)	0.037
*D** in PaB	-0.521 (-3.056, 0.393)	0.815	-0.023 (-1.636, 0.587)	0.519	-0.256 (-2.207, 0.491)	0.691
f in PaB	0.385 (-0.407, 0.739)	0.124	-0.087 (-1.441, 0.534)	0.580	-0.332 (-2.715, 0.515)	0.748
D in PaT	0.324 (-0.614, 0.718)	0.186	0.286 (-0.557, 0.69)	0.201	0.908 (0.781, 0.961)	< 0.001
*D** in PaT	0.569 (-0.204, 0.836)	0.060	-0.289 (-2.251, 0.475)	0.713	-0.062 (-1.02, 0.504)	0.569
f in PaT	0.531 (-0.144, 0.806)	0.047	0.35 (-0.633, 0.735)	0.174	0.486 (-0.275, 0.789)	0.073
SNR	0.081 (-0.206, 0.421)	0.312	0.178 (-0.238, 0.551)	0.205	0.067 (-0.152, 0.364)	0.301
ADC value	0.870 (0.691, 0.946)	< 0.001	0.707 (0.393, 0.871)	< 0.001	0.808 (0.590, 0.917)	< 0.001

ICC: Intraclass correlation coefficient; SNR: Signal-to-noise ratio; PaH: Pancreatic head; ADC: Apparent diffusion coefficient; *D*: Diffusion coefficient; PaT: Pancreatic tail; PaB: Pancreatic body; *f*: Perfusion fraction; *D**: False diffusion coefficient.

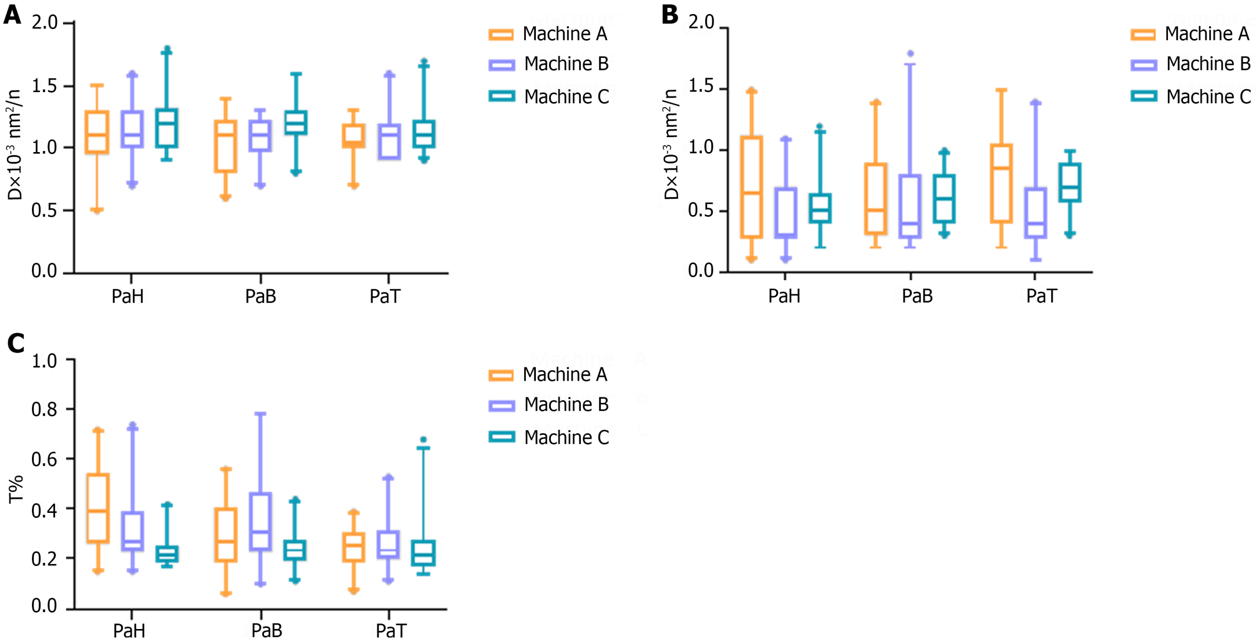

Figure 1 True diffusion coefficient, false diffusion coefficient, and perfusion fraction values of the pancreatic head, body, and tail on different devices. A: True diffusion coefficient values; B: False diffusion coefficient values; C: Perfusion fraction values. PaH: Pancreas head; PaB: Pancreas body; PaT: Pancreas tail; *D*: True diffusion coefficient; *f*: Perfusion fraction; *D**: False diffusion coefficient.

In our study, the kappa coefficient for subjective image quality assessment at b = 1200 s/mm^2 among different observers was 0.776, indicating a good consistency in subjective image quality ratings. The ICC for all the quantitative parameter values between different observers was 0.803, and the quantitative parameter value measured by the same observer on two different occasions was 0.883. Notably, both ICCs were > 0.75, indicating excellent consistency in the measurements of the quantitative parameter values among different observers and within the same observer across the two measurements.

We used images acquired at b = 0 and b = 1200 s/mm^2 to analyze the ADC values between different devices. The ICC values for pairwise comparisons between different devices were 0.870, 0.707, and 0.808, respectively, indicating good consistency among the three devices. This finding is consistent with the results of previous studies[18,19]. However, the ICC statistical analysis of the SNR between different machines yielded P > 0.05, indicating no statistical significance. This could be attributed to differences in imaging parameters used by different devices during image acquisition.

Table 3 Comparison of diffusion coefficient, false diffusion coefficient, and perfusion fraction values of the pancreatic head, body, and tail measured using machines A, B, and C

Region and parameter	Machine A	Machine B	Machine C	Mixed liner model		*Post-hoc* test		95% limits of agreement
				F	*P* value	Pair comparison	P^1 value	
PaH								
D	1.08 ± 0.27	1.15 ± 0.22	1.22 ± 0.23	2.893	0.078	A *vs* B	0.986	-0.56, 0.38
						A *vs* C	0.140	-0.47, 0.44
						B *vs* C	0.311	-0.32, 0.27
*D**	0.07 ± 0.04	0.05 ± 0.03	0.05 ± 0.02	2.275	0.128	A *vs* B	0.139	-0.13, 0.03
						A *vs* C	0.327	-0.11, 0.03
						B *vs* C	0.531	-0.05, 0.04
f	0.40 ± 0.18	0.33 ± 0.15	0.23 ± 0.07	15.725	0.001	A *vs* B	0.483	-0.57, 0.16
						A *vs* C	0.001	-0.52, 0.00
						B *vs* C	0.030	-0.40, 0.06
PaB								
D	1.05 ± 0.24	1.09 ± 0.18	1.21 ± 0.20	10.060	0.001	A *vs* B	0.999	-0.46, 0.27
						A *vs* C	0.003	-0.21, 0.33
						B *vs* C	0.027	-0.27, 0.31
*D**	0.06 ± 0.04	0.05 ± 0.04	0.06 ± 0.02	0.228	0.798	A *vs* B	0.999	-0.12, 0.05
						A *vs* C	0.999	-0.08, 0.04
						B *vs* C	0.999	-0.09, 0.05
f	0.30 ± 0.15	0.37 ± 0.20	0.24 ± 0.07	3.174	0.062	A *vs* B	0.513	-0.36, 0.27
						A *vs* C	0.420	-0.39, 0.11
						B *vs* C	0.066	-0.57, 0.10
PaT								
D	1.07 ± 0.16	1.12 ± 0.22	1.15 ± 0.18	2.438	0.112	A *vs* B	0.999	-0.42, 0.28
						A *vs* C	0.258	-0.34, 0.29
						B *vs* C	0.601	-0.19, 0.14
*D**	0.08 ± 0.04	0.05 ± 0.03	0.07 ± 0.02	9.451	0.001	A *vs* B	0.002	-0.10, 0.00
						A *vs* C	0.999	-0.11, 0.04
						B *vs* C	0.058	-0.06, 0.06
f	0.25 ± 0.08	0.26 ± 0.10	0.25 ± 0.12	0.191	0.827	A *vs* B	0.999	-0.20, 0.12
						A *vs* C	0.999	-0.25, 0.13
						B *vs* C	0.999	-0.27, 0.12

[1]The Bonferroni method was used to adjust the *P* value. The adjusted *P* value was equal to the original *P* value multiplied by 3. PaH: Pancreatic head; ADC: Apparent diffusion coefficient; *D*: Diffusion coefficient; PaT: Pancreatic tail; PaB: Pancreatic body; *f*: Perfusion fraction; *D**: False diffusion coefficient.

In the consistency analysis of various IVIM parameter values, devices A and B showed statistical significance only for the *f* value of the PaT region, with an ICC of 0.531. Devices A and C exhibited statistical significance only for the *D* value of the PaB region, with an ICC value of 0.683. The remaining parameters between devices A and B and between devices A and C showed no statistically significant differences, indicating poor repeatability between devices A and B and between devices A and C. Devices B and C showed a statistical difference in the *D* and *D** values in the PaH region, the *D* value in the PaB region, and the *D* value in the PaT region, with an ICC of 0.728, 0.578, 0.551, and 0.908, respectively. This indicates that the consistency between devices B and C was better than that between devices A and B and between devices A and C, and the repeatability of the *D* values in different pancreatic regions between devices B and C was relatively good. Considering the magnitude of the ICC among the statistically significant parameters mentioned above,

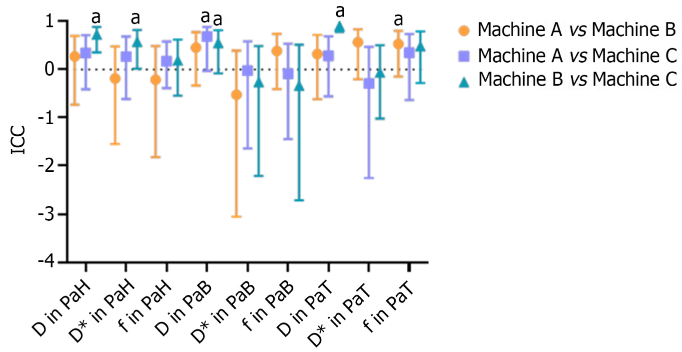

Figure 2 Intraclass correlation coefficient map of pairwise comparison between different machines in different parts of the pancreas. [a]*P* < 0.05. ICC: Intraclass correlation coefficient; PaH: Pancreas head; PaB: Pancreas body; PaT: Pancreas tail; *D*: True diffusion coefficient; *f*: Perfusion fraction; *D*∗: False diffusion coefficient.

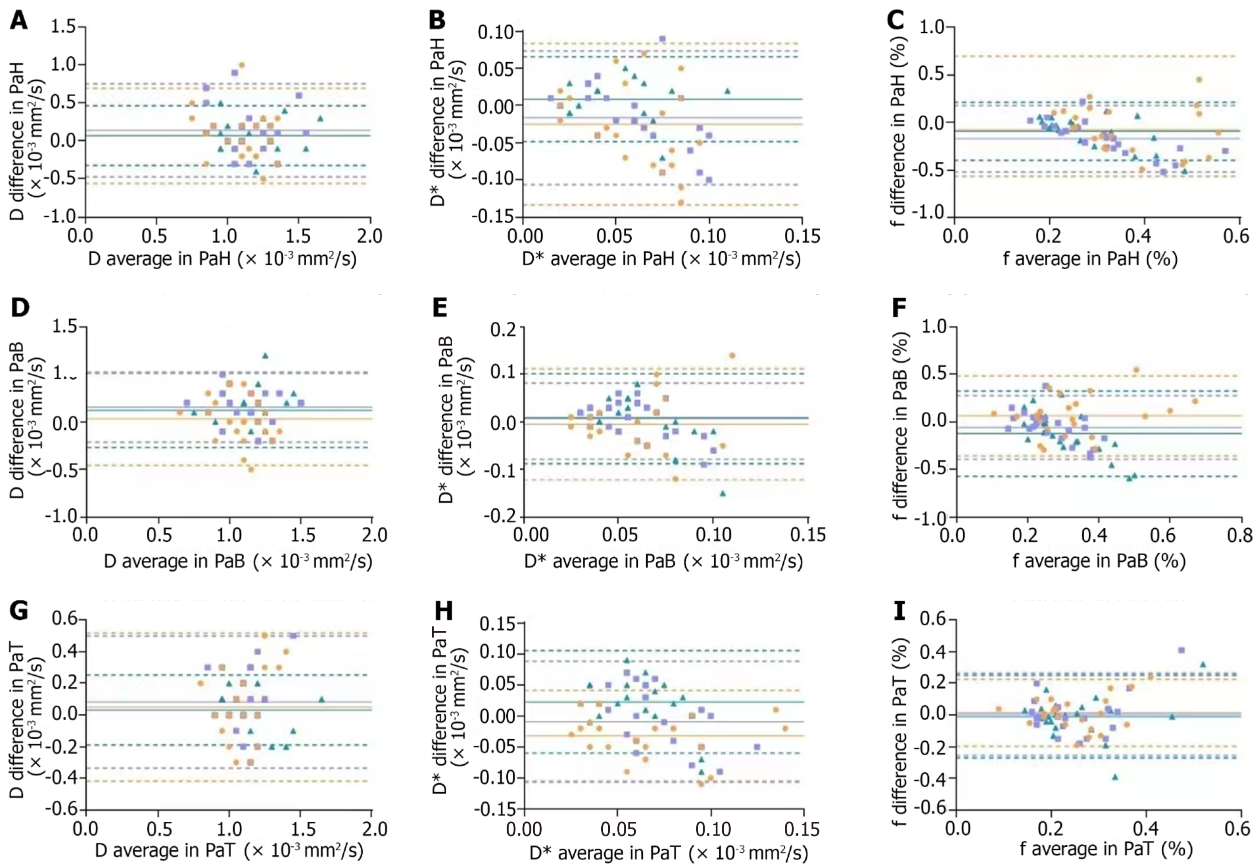

Figure 3 Comparison of consistency of true diffusion coefficient, false diffusion coefficient, and perfusion fraction values measured using different machines. A: True diffusion coefficient (*D*) average in pancreatic head (PaH); B: False diffusion coefficient (*D*∗) average in PaH; C: Perfusion fraction (*f*) average in PaH; D: *D* average in pancreatic body (PaB); E: *D*∗ average in PaB; F: *f* average in PaB; G: *D* average in pancreatic tail (PaT); H: *D*∗ average in PaT; I: *f* average in PaT.

only the ICC for the *D* value in the PaT region between devices B and C was > 0.75. The ICC for the other parameters was between 0.4 and 0.75, indicating some consistency between devices B and C; however, the degree of consistency was mostly moderate and did not reach a high level of agreement.

In the mixed linear model, when $P < 0.05$, a significant difference exists between the two data sets. According to the results of statistical analysis, there were differences in the IVIM parameters between different machines in the PaH (*f* value), PaB (*D* value), and PaT regions (*D*∗ value). Machine C had a lower *f* value in the PaH region than machines A and B. Machine C had a higher *D* value in the PaB region than machines A and B. Machine B had a lower *D*∗ value in the PaT region than the other machines. This may have been associated with using different post-processing software and algorithms in the IVIM numerical analysis on different machines.

Based on the Bland-Altman plot results for different machines, the approximate distribution of different parameters could be visually observed. These plots showed that only 1-2 data points fell outside the dashed lines (representing the 95%CI), indicating that only a few parameters had relatively large variability, whereas most parameters exhibited acceptable consistency. However, considering the statistical analysis results mentioned earlier, it should be noted that many IVIM parameters had ICC values that are not particularly high, and significant differences existed in some parameter values. In summary, the repeatability of the IVIM parameter values between different devices appeared to be moderate.

This study had some limitations. First, our study only included data from the pancreas of young and middle-aged individuals and did not include individuals of other age groups. However, the extended duration of the examination may have been challenging for children and older adults to endure, making them unable to complete all examination procedures. In addition, images of patients with lesions were not incorporated in our study. In clinical practice, patients with pancreatic cancer often have compromised health, and it can be challenging for them to undergo examinations simultaneously using three different devices. Moreover, there could have been a selection bias if patients with benign pancreatic lesions were selected.

Furthermore, we used MITK-diffusion post-processing software from different manufacturers for IVIM analysis. Therefore, while we could ensure consistency in ROI sizes between different devices, the ROI positions could only be approximately matched. This may have introduced some bias into the measurements. In addition, the lack of uniformity in the post-processing software could introduce variations in the algorithms used, potentially affecting the final results. In such cases, it is possible to standardize the differences between MRI devices through phantom calibration, which can then be used to correct the results. However, it is crucial to note that using phantoms for calibration inevitably increases the time and economic costs associated with the study.

CONCLUSION

Pancreatic scans were conducted in volunteers using different MRI devices, and we found that the variability in IVIM parameter values may be associated with using various MRI equipment. The consistency of the ADC values between different devices was good; however, the overall repeatability of the IVIM parameter values was moderate. Therefore, applying IVIM parameter values in diagnosing pancreatic cancer should be approached cautiously.

FOOTNOTES

Author contributions: Liu X, Wang YF, and Wang Q designed the research study; Qi XH, Zhang ZL, Pan JY, and Fan XL performed the research; Du Y and Zhai YM contributed analytic tools; Liu X, Wang YF, and Wang Q analyzed the data and wrote the manuscript; all authors have read and approved the final manuscript.

Supported by The Fourth Hospital of Hebei Medical University, No. 20210423.

Institutional review board statement: This study was approved by the institutional review board of The Fourth Hospital of Hebei Medical University.

Informed consent statement: Informed consent was obtained from all participants.

Conflict-of-interest statement: There is no conflict of interest to disclose.

Data sharing statement: The data are available from the corresponding author upon reasonable request.

Country of origin: China

ORCID number: Qi Wang 0009-0005-7042-0646.

S-Editor: Qu XL
L-Editor: Wang TQ
P-Editor: Cai YX

REFERENCES

1 **Le Bihan D**, Breton E, Lallemand D, Aubin ML, Vignaud J, Laval-Jeantet M. Separation of diffusion and perfusion in intravoxel incoherent

motion MR imaging. *Radiology* 1988; **168**: 497-505 [PMID: 3393671 DOI: 10.1148/radiology.168.2.3393671]
2 **Le Bihan D**, Breton E, Lallemand D, Grenier P, Cabanis E, Laval-Jeantet M. MR imaging of intravoxel incoherent motions: application to diffusion and perfusion in neurologic disorders. *Radiology* 1986; **161**: 401-407 [PMID: 3763909 DOI: 10.1148/radiology.161.2.3763909]
3 **Englund EK**, Berry DB, Behun JJ, Ward SR, Frank LR, Shahidi B. IVIM Imaging of Paraspinal Muscles Following Moderate and High-Intensity Exercise in Healthy Individuals. *Front Rehabil Sci* 2022; **3** [PMID: 35959464 DOI: 10.3389/fresc.2022.910068]
4 **Markiet K**, Glinska A, Nowicki T, Szurowska E, Mikaszewski B. Feasibility of Intravoxel Incoherent Motion (IVIM) and Dynamic Contrast-Enhanced Magnetic Resonance Imaging (DCE-MRI) in Differentiation of Benign Parotid Gland Tumors. *Biology (Basel)* 2022; **11** [PMID: 35336773 DOI: 10.3390/biology11030399]
5 **Yang D**, She H, Wang X, Yang Z, Wang Z. Diagnostic accuracy of quantitative diffusion parameters in the pathological grading of hepatocellular carcinoma: A meta-analysis. *J Magn Reson Imaging* 2020; **51**: 1581-1593 [PMID: 31654537 DOI: 10.1002/jmri.26963]
6 **Zhang Y**, Kuang S, Shan Q, Rong D, Zhang Z, Yang H, Wu J, Chen J, He B, Deng Y, Roberts N, Shen J, Venkatesh SK, Wang J. Can IVIM help predict HCC recurrence after hepatectomy? *Eur Radiol* 2019; **29**: 5791-5803 [PMID: 30972544 DOI: 10.1007/s00330-019-06180-1]
7 **Yoon JH**, Lee JM, Lee KB, Kim SW, Kang MJ, Jang JY, Kannengiesser S, Han JK, Choi BI. Pancreatic Steatosis and Fibrosis: Quantitative Assessment with Preoperative Multiparametric MR Imaging. *Radiology* 2016; **279**: 140-150 [PMID: 26566228 DOI: 10.1148/radiol.2015142254]
8 **Lemke A**, Laun FB, Klauss M, Re TJ, Simon D, Delorme S, Schad LR, Stieltjes B. Differentiation of pancreas carcinoma from healthy pancreatic tissue using multiple b-values: comparison of apparent diffusion coefficient and intravoxel incoherent motion derived parameters. *Invest Radiol* 2009; **44**: 769-775 [PMID: 19838121 DOI: 10.1097/RLI.0b013e3181b62271]
9 **Warmuth-metz M**. Imaging Differential Diagnosis of Pediatric CNS Tumors. *Imaging Diagn Pediatric Brain Tumor Stud* 2017 [DOI: 10.1007/978-3-319-42503-0_3]
10 **Kim B**, Lee SS, Sung YS, Cheong H, Byun JH, Kim HJ, Kim JH. Intravoxel incoherent motion diffusion-weighted imaging of the pancreas: Characterization of benign and malignant pancreatic pathologies. *J Magn Reson Imaging* 2017; **45**: 260-269 [PMID: 27273754 DOI: 10.1002/jmri.25334]
11 **Ma W**, Wei M, Han Z, Tang Y, Pan Q, Zhang G, Ren J, Huan Y, Li N. The added value of intravoxel incoherent motion diffusion weighted imaging parameters in differentiating high-grade pancreatic neuroendocrine neoplasms from pancreatic ductal adenocarcinoma. *Oncol Lett* 2019; **18**: 5448-5458 [PMID: 31612053 DOI: 10.3892/ol.2019.10863]
12 **Bian H**, Liu F, Chen S, Li G, Song Y, Sun M, Dong H. Intravoxel incoherent motion diffusion-weighted imaging evaluated the response to concurrent chemoradiotherapy in patients with cervical cancer. *Medicine (Baltimore)* 2019; **98**: e17943 [PMID: 31725650 DOI: 10.1097/MD.0000000000017943]
13 **Ma C**, Liu L, Li YJ, Chen LG, Pan CS, Zhang Y, Wang H, Chen SY, Lu JP. Intravoxel incoherent motion MRI of the healthy pancreas: Monoexponential and biexponential apparent diffusion parameters of the normal head, body and tail. *J Magn Reson Imaging* 2015; **41**: 1236-1241 [PMID: 24979657 DOI: 10.1002/jmri.24684]
14 **Kang KM**, Lee JM, Yoon JH, Kiefer B, Han JK, Choi BI. Intravoxel incoherent motion diffusion-weighted MR imaging for characterization of focal pancreatic lesions. *Radiology* 2014; **270**: 444-453 [PMID: 24126370 DOI: 10.1148/radiol.13122712]
15 **Ding X**, Xu J, Zhou J, Long Q, Xu H. Effects of different breathing techniques on the IVIM-derived quantitative parameters of the normal pancreas. *Eur J Radiol* 2021; **143**: 109892 [PMID: 34388419 DOI: 10.1016/j.ejrad.2021.109892]
16 **Merisaari H**, Toivonen J, Pesola M, Taimen P, Boström PJ, Pahikkala T, Aronen HJ, Jambor I. Diffusion-weighted imaging of prostate cancer: effect of b-value distribution on repeatability and cancer characterization. *Magn Reson Imaging* 2015; **33**: 1212-1218 [PMID: 26220861 DOI: 10.1016/j.mri.2015.07.004]
17 **Wáng YXJ**, Wang X, Wu P, Wang Y, Chen W, Chen H, Li J. Topics on quantitative liver magnetic resonance imaging. *Quant Imaging Med Surg* 2019; **9**: 1840-1890 [PMID: 31867237 DOI: 10.21037/qims.2019.09.18]
18 **Donati OF**, Chong D, Nanz D, Boss A, Froehlich JM, Andres E, Seifert B, Thoeny HC. Diffusion-weighted MR imaging of upper abdominal organs: field strength and intervendor variability of apparent diffusion coefficients. *Radiology* 2014; **270**: 454-463 [PMID: 24471390 DOI: 10.1148/radiol.13130819]
19 **Barral M**, Soyer P, Ben Hassen W, Gayat E, Aout M, Chiaradia M, Rahmouni A, Luciani A. Diffusion-weighted MR imaging of the normal pancreas: reproducibility and variations of apparent diffusion coefficient measurement at 1.5- and 3.0-Tesla. *Diagn Interv Imaging* 2013; **94**: 418-427 [PMID: 23415463 DOI: 10.1016/j.diii.2012.12.007]

Published by **Baishideng Publishing Group Inc**
7041 Koll Center Parkway, Suite 160, Pleasanton, CA 94566, USA
Telephone: +1-925-3991568
E-mail: office@baishideng.com
Help Desk: https://www.f6publishing.com/helpdesk
https://www.wjgnet.com